

Spring 4-23-2016

Hiding inside? Intracellular expression of non-glycosylated c-kit protein in cardiac progenitor cells

Huilin Shi

Christopher A. Drummond

Xiaoming Fan

Steven T. Haller

Jiang Liu

Marshall University, liuj@marshall.edu

See next page for additional authors

Follow this and additional works at: http://mds.marshall.edu/sp_psr

 Part of the [Medical Sciences Commons](#), and the [Pharmacy and Pharmaceutical Sciences Commons](#)

Recommended Citation

Shi H, Drummond CA, Fan X, et al. Hiding inside? Intracellular expression of non-glycosylated c-kit protein in cardiac progenitor cells. *Stem Cell Research*. 2016;16(3):795-806. doi:10.1016/j.scr.2016.04.017.

This Article is brought to you for free and open access by the Faculty Research at Marshall Digital Scholar. It has been accepted for inclusion in Pharmaceutical Science and Research by an authorized administrator of Marshall Digital Scholar. For more information, please contact zhangj@marshall.edu, martj@marshall.edu.

Authors

Huilin Shi, Christopher A. Drummond, Xiaoming Fan, Steven T. Haller, Jiang Liu, Deepak Malhotra, and Jiang Tian



Hiding inside? Intracellular expression of non-glycosylated c-kit protein in cardiac progenitor cells



Huilin Shi^a, Christopher A. Drummond^a, Xiaoming Fan^a, Steven T. Haller^a, Jiang Liu^b, Deepak Malhotra^a, Jiang Tian^{a,*}

^a Department of Medicine, Division of Cardiovascular Medicine, College of Medicine and Life Sciences, University of Toledo, Toledo, OH 43614, USA

^b Joan C. Edwards School of Medicine, Marshall University, Huntington, WV 25755, USA

ARTICLE INFO

Article history:

Received 25 January 2016
Received in revised form 15 April 2016
Accepted 22 April 2016
Available online 23 April 2016

Keywords:

C-kit
Cardiac progenitor cell
Glycosylation
Endothelial differentiation

ABSTRACT

Cardiac progenitor cells including c-kit⁺ cells and cardiosphere-derived cells (CDCs) play important roles in cardiac repair and regeneration. CDCs were reported to contain only small subpopulations of c-kit⁺ cells and recent publications suggested that depletion of the c-kit⁺ subpopulation of cells has no effect on regenerative properties of CDCs. However, our current study showed that the vast majority of CDCs from murine heart actually express c-kit, albeit, in an intracellular and non-glycosylated form. Immunostaining and flow cytometry showed that the fluorescent signal indicative of c-kit immunostaining significantly increased when cell membranes were permeabilized. Western blots further demonstrated that glycosylation of c-kit was increased during endothelial differentiation in a time dependent manner. Glycosylation inhibition by 1-deoxymannojirimycin hydrochloride (1-DMM) blocked c-kit glycosylation and reduced expression of endothelial cell markers such as Flk-1 and CD31 during differentiation. Pretreatment of these cells with a c-kit kinase inhibitor (imatinib mesylate) also attenuated Flk-1 and CD31 expression. These results suggest that c-kit glycosylation and its kinase activity are likely needed for these cells to differentiate into an endothelial lineage. In vivo, we found that intracellular c-kit expressing cells are located in the wall of cardiac blood vessels in mice subjected to myocardial infarction. In summary, our work demonstrated for the first time that c-kit is not only expressed in CDCs but may also directly participate in CDC differentiation into an endothelial lineage.

© 2016 The Authors. Published by Elsevier B.V. This is an open access article under the CC BY-NC-ND license (<http://creativecommons.org/licenses/by-nc-nd/4.0/>).

1. Introduction

Studies have shown that progenitor cells exist in adult hearts, including aged and diseased hearts (Mercola et al., 2011; Olson and Schneider, 2003). Different types of cardiac progenitor cells were discovered including c-kit⁺, Sca-1⁺, Islet-1⁺, SSEA-1⁺ cells, as well as side population and cardiosphere-derived cells (CDCs) (Nigro et al., 2015). Animal and clinical studies have shown that c-kit⁺ cells and CDCs play important roles in cardiac repair and regeneration (Leri et al., 2015; Marban and Cingolani, 2012; Ellison et al., 2013; Hariharan et al., 2015; Fransioli et al., 2008). C-kit⁺ progenitor cells were first identified in rat cardiac tissues (Beltrami et al., 2003). Despite debate on the role of c-kit⁺ cells in myogenesis (Leri et al., 2015; Goldstein et al., 2015; van Berlo et al., 2014), c-kit protein expression is the most recognized progenitor cell marker. CDCs were initially isolated from human and murine cardiac tissue (Messina et al., 2004) and

were introduced as a candidate progenitor cell for regenerative therapy after myocardial infarction (MI) (Smith et al., 2007). Clinical trials such as CADUCEUS (Makkar et al., 2012) demonstrated that injection of CDCs improved cardiac function and increased viable tissue in patients with MI. Finally, it was reported that CDCs contain a small subpopulation of c-kit⁺ cells, ranging from ~1% to ~25% (Messina et al., 2004; Smith et al., 2007; Cheng et al., 2014).

C-kit protein, first identified as a virus proto-oncogene, v-kit (Besmer et al., 1986), is a tyrosine kinase and a receptor for stem cell factor (SCF), containing nine N-glycosylation sites in its sequence (Nigro et al., 2015; Yarden et al., 1987). It is known that c-kit undergoes N-linked glycosylation in the endoplasmic reticulum (ER) before being transported to the Golgi apparatus where it is modified by further complex glycosylations and subsequently transported to the cell surface (Aebi, 2013). Two forms of c-kit protein, a non-glycosylated form (~100–120 kDa) and a glycosylated form (~140 kDa), were detected previously in cancer cells (Blume-Jensen et al., 1991; Rubin et al., 2001; Schmidt-Arras et al., 2005). In studies of cardiac progenitor cells, cellular distribution and glycosylation of c-kit have not been evaluated.

Increased c-kit⁺ cell number was observed in different disease states, and conditional knockout of c-kit was found to abolish cardiac

* Corresponding author at: University of Toledo, College of Medicine and Life Sciences, Department of Medicine, Cardiology Division, Health Science Campus, Mail Stop 1025, 3000 Arlington Ave., Toledo, OH 43614-2598, USA.
E-mail address: Jiang.Tian@utoledo.edu (J. Tian).

regeneration in experimental heart failure (Ellison et al., 2013; Ellison et al., 2007). Our previous study also showed that c-kit⁺ cells were increased in cardiac tissue from mice with chronic kidney disease, particularly in transgenic mice with reduced Na/K-ATPase- α mediated signaling capability (Drummond et al., 2014). However, the specific role of c-kit protein and its regulatory mechanism in these progenitor cells remain elusive. The current work studied c-kit expression and its potential role in cardiac progenitor cell differentiation into an endothelial lineage.

2. Materials and methods

2.1. Animals

Animal experiments were conducted in accordance with the National Institutes of Health, Guide for the Care and Use of Laboratory Animals under protocols approved by the Institutional Animal Care and Use Committee at the University of Toledo. Mice from an inbred C57BL6/J strain (Moseley et al., 2004) were maintained at the University of Toledo. Adult male mice which were two months of age were used for isolation of cardiosphere-derived progenitor cells and for myocardial infarction experiments.

2.2. Isolation of cardiac progenitor cells

Cardiosphere-derived cells (CDCs) were obtained following procedures previously described (Messina et al., 2004; Smith et al., 2007) with minor modifications. Briefly, gross connective tissue was removed by blunt dissection to obtain pure mouse heart muscle tissue, which was then cut into small explants (~1 mm in dimension). The explants were washed and partially digested enzymatically with 0.025% Trypsin/0.01% ethylenediaminetetraacetic acid (EDTA, Gibco Inc., Grand Island, NY, Cat. No.: R001-100) for 10 min. The explants were then cultured on dishes coated with fibronectin (Santa Cruz Inc., Santa Cruz, CA, Cat. No.: sc-29011) in complete explant medium (CEM), which contains: 500 mL Iscove's Modified Dulbecco's Medium (IMDM, Gibco Inc., Cat. No.: 12440), 125 mL Fetal bovine serum (FBS) (Gibco Inc., Cat. No.: 10437), 1% penicillin–streptomycin (Mediatech Inc., Manassas, VA, Cat. No.: 30-002-CI), 1 mmol/L L-glutamine (Gibco Inc., Cat. No.: 25030), and 1 mmol/L 2-mercaptoethanol (Sigma-Aldrich, St. Louis, MO, Cat. No.: M6250). After 14 days, a layer of stromal-like cells grew out of adherent explants, over which small, round, phase-bright cells migrated. These phase-bright cells were harvested by sequential Versene (Gibco Inc., Cat. No.: 15040) and 0.025% Trypsin-0.01% EDTA digestion and seeded on poly-D-lysine coated (Sigma-Aldrich, Cat. No.: P6407) dishes in cardiosphere growth medium (CGM) that contains: 175 mL IMDM, 325 mL DMEM/F12 (Gibco Inc., Cat. No.: 11330), 3.5% FBS, 1% penicillin–streptomycin, 1 mmol/L L-glutamine, 2% B27 supplement (Gibco Inc., Cat. No.: 17504), 1 mmol/L 2-mercaptoethanol, 80 ng/mL basic Fibroblast growth factor (bFGF, PeproTech Inc., Rocky Hill, NJ, Cat. No.: AF-450-33), 25 ng/mL epidermal growth factor (EGF, PeproTech Inc., Cat. No.: 315-09), 4 ng/mL cardiotrophin-1 (PeproTech Inc., Cat. No.: 250-25), 1 unit/mL α -Thrombin (Haemtech Inc., Essex Junction, VT, Cat. No.: HCT-0020). The seeded cells formed cardiospheres on poly-D-lysine coated dishes following 7 to 21 days. Subsequently, the cardiosphere forming cells were collected and plated on fibronectin-coated dishes in CGM where they expand as monolayers. CDCs were expanded and stocks were collected and stored in liquid nitrogen for later experiments.

2.3. Inducing endothelial lineage differentiation of CDCs

CDCs at the 5th–15th passages were used for endothelial differentiation. CDCs were seeded on matrigel-coated dishes or glass coverslips. For Western blotting, CDCs grew in CGM for three days at which time they reached 80% confluence. Then media was changed to complete

mouse endothelial cell culture medium (MECM, Cell Biologics Inc., Chicago, IL, Cat. No.: M1168) to start endothelial differentiation. For immunostaining, CDCs were allowed to attach to coverslips in CGM overnight, at which point the media was changed to MECM to start endothelial differentiation. MECM was changed every two days during differentiation until cells were collected for Western blot or immunostaining. Following the start of endothelial differentiation cells were collected on days 1, 3, 7, 10, 14, 21, and 28.

For inhibition of N-glycosylation in CDCs, 1-deoxymannojirimycin hydrochloride (1-DMM, Sigma-Aldrich, Cat. No.: D9160), an inhibitor of N-linked glycosylation, was added to MECM at 5, 50 and 500 μ M concentrations during induction of endothelial differentiation. CDCs in MECM without 1-DMM were used as control. The induction media was changed every two days. Cells were collected on day 7 and 14 for Western blot.

Specific inhibition of c-kit kinase activity was achieved through the use of the c-kit tyrosine kinase inhibitor imatinib mesylate (Selleckchem, Cat. No.: S1026) which was added to MECM at 0.1, 0.2, 0.5, 1, 2, 5, and 10 μ M concentrations during the 14 day endothelial differentiation induction period. Cells treated with MECM alone without imatinib mesylate were used as controls. The induction media was changed every two days. Cells were collected on day 14 for Western blot.

2.4. Immunocytochemistry

Cells were fixed in 3% paraformaldehyde. Following fixation, cells were washed with 1 \times Dulbecco's phosphate buffered saline (DPBS; Gibco, Cat. No.: 14190-144) three times and were then blocked with 2% Bovine Serum Albumin (BSA; Sigma-Aldrich Inc., Cat. No.: A4503) in DPBS containing 0.3% Triton X-100 (DPBS-Tr) for 1 h at room temperature. Subsequently, cells were incubated with primary antibodies diluted in blocking buffer in a humidified chamber overnight at 4 $^{\circ}$ C. The next day, cells were washed three times with DPBS-Tr. Cells were then incubated with secondary antibodies diluted in blocking buffer at room temperature for 1.5 h. Following incubation with secondary antibody, the cells were washed with DPBS-Tr one time. Cells were then incubated with 4',6-diamidino-2-phenylindole (DAPI, Life Technologies Inc., Cat. No.: D1306) solution for 5 min and were washed three times in DPBS-Tr. The coverslips were then mounted with Prolong Gold anti-fade reagent (Life Technologies Inc., Cat. No.: 36,930). Immunofluorescence was visualized on a confocal microscope (TCS SP5 LCSM, Leica, Buffalo Grove, IL).

The primary antibodies used in immunostaining include: anti-c-kit-FITC antibody, 1:100 dilution (Abcam Inc., Cambridge, MA, Cat. No.: ab24870); rabbit anti-CD31, 1:20 dilution (Abcam Inc., Cat. No.: ab28364); mouse anti-Flk-1, 1:50 dilution (Santa Cruz Inc., Cat. No.: sc-6251); rat anti-CD90, 1:100 dilution (Abcam Inc., Cat. No.: ab3105); rat anti-mouse CD105, 1:50 dilution (R&D Systems, Minneapolis, MN, Cat. No.: MAB1320); rabbit anti-Oct3/4, 1:200 dilution (Santa Cruz Inc., Cat. No.: sc-9081); rabbit anti-Nanog, 1:200 dilution (Santa Cruz Inc., Cat. No.: sc-33760); rabbit anti-Nkx2.5, 1:400 dilution (Abcam Inc., Cat. No.: ab22611); rabbit anti-GATA4, 1:200 dilution (Santa Cruz Inc., Cat. No.: sc-9053); mouse anti- α -actinin, 1:1000 dilution (Sigma-Aldrich Inc., Cat. No.: A7811); rabbit anti-cardiac troponin I, 1:100 dilution (Abcam Inc., Cat. No.: ab47003); rabbit anti- α -smooth muscle actin, 1:500 dilution (Abcam Inc., Cat. No.: ab5694); chicken anti-vimentin, 1:200 dilution (Abcam Inc., Cat. No.: ab24525); rat anti-mouse CD31, 1:100 dilution (AbD Serotec Inc., Cat. No.: MCA2388GA). The secondary antibodies included: goat anti-rabbit IgG (H + L), Alexa Fluor 594 conjugate (Life Technologies Inc., Cat. No.: A-11012); goat anti-mouse IgG (H + L), Alexa Fluor 594 conjugate (Life Technologies Inc., Cat. No.: A-11005); goat anti-mouse IgG (H + L), Alexa Fluor 488 conjugate (Life Technologies Inc., Cat. No.: A-11001); goat anti-rat IgG (H + L), Alexa Fluor 488 conjugate (Life Technologies Inc., Cat. No.: A-11006); goat anti-chicken IgG (H + L), Alexa Fluor 647 conjugate

(Life Technologies Inc., Cat. No.: A-21449). Secondary antibodies were all used at 1:600–1:800 dilutions.

2.5. Flow cytometry

CDCs were grown in a fibronectin-coated 75 cm² flask. Once the cells reached 80% confluence they were collected and prepared for flow cytometry, briefly as follows: CDCs were washed with DPBS twice, then incubated with 5 mL Versene at 37 °C with 5% CO₂ for 10 min. Detached cells were suspended in CGM and centrifuged at 2000 × g for 5 min. Pelleted cells were washed once with 12 mL FACS buffer (DPBS containing 2% BSA). Washed cells were then suspended in 3 mL of 1.5% paraformaldehyde solution and rotated at room temperature for 10 min for fixation. Following fixation cells were washed once with 12 mL FACS buffer and suspended in fresh FACS buffer. For membrane permeabilization, fixed cells were incubated with FACS buffer containing 0.1% Triton X-100 for 5 min. Anti-c-kit-FITC antibody (Abcam Inc., Cat. No.: ab24870), 1:200 dilution, was then added to the cell suspension and incubated on ice for 30 min in the dark. Non-permeabilized cells were directly incubated with antibody without Triton X-100. After antibody incubation, cells were washed twice with FACS buffer and resuspended in 1 mL FACS buffer. Flow cytometry was performed on a Becton-Dickinson FACSCalibur Flow Cytometer (Becton-Dickinson, San Jose, CA). Cells that were not permeabilized and not incubated with antibody were used as negative control.

2.6. RNA isolation and reverse transcription-quantitative polymerase chain reaction (RT-qPCR)

CDCs were collected in 350 µL of lysis buffer RLT to begin isolation of total RNA using the RNeasy mini kit (Qiagen Inc., Carol Stream, IL, Cat. No.: 217004), according to the instructions provided by the manufacturer. Immediately following RNA isolation, cDNA was synthesized for mRNA briefly as follows: cDNA was synthesized using the RT² First Strand cDNA Synthesis Kit from Qiagen according to the manufacturer's protocol using 1 µg total RNA as input (Qiagen Inc., Cat. No.: 330404). Following reverse transcription cDNA was diluted according to the manufacturer's protocol for storage at –20 °C and later use in qPCR.

To determine the level of c-kit gene expression, Gapdh was used as an internal control. We also compared the expression of c-kit with Na/K-ATPase α1 gene (Atp1a1), a ubiquitously expressed gene in all mammalian cells. RT² qPCR primer assays for mouse c-kit (Cat. No.: PPM05195A-200), Atp1a1 (Cat. No.: PPM04163A-200), and Gapdh (Cat. No.: PPM02946E-200) were purchased from Qiagen Inc. and were used in the RT² SYBR Green qPCR reaction mix (Qiagen Inc., Cat. No.: 330529) according to the manufacturer's protocol. Reactions were carried out on an ABI 7500 Fast platform (Life Technologies, Boston, MA) using the following cycling program: 10 min incubation at 95 °C, [95 °C for 15 s, 60 °C for 1 min (Fluorescence detection performed)] repeated 40 times. A determination of mRNA expression was conducted by comparing the relative change in cycle threshold value (ΔCt) from the internal control, GAPDH.

2.7. Western blot analysis

Western blots were carried out as described previously (Drummond et al., 2014; Elkareh et al., 2007; Li et al., 2011). Cell lysates were collected in radio-immunoprecipitation assay (RIPA) buffer (Santa Cruz Inc., Cat. No.: sc-24948) containing protease inhibitors and phosphatase inhibitors. Electrophoretic separation of protein was performed on 8% Tris/glycine SDS-polyacrylamide gels and separated proteins were then transferred to 0.45 µm nitrocellulose blotting membrane. Membranes were blocked with 5% non-fat dry milk or 5% BSA for 1 h at room temperature. Membranes were then incubated with specific primary antibodies suspended in blocking buffer

overnight at 4 °C. After washing, membranes were incubated with appropriate secondary antibodies. Clarity Western ECL substrate (Bio-Rad Inc., Cat. No.: 170-5060) was used for chemiluminescence detection on an Omega Lum™ G imaging system (Aplegen Inc., San Francisco, CA).

The primary antibodies used in Western blot analyses were: rabbit anti-c-kit antibody, 1:500 dilution (Abcam Inc., Cat. No.: ab5506); rat anti-mouse CD31, 1:1000 dilution (AbD Serotec Inc., Raleigh, NC, Cat. No.: MCA2388GA); mouse anti-Flk-1, 1:1000 dilution (Santa Cruz Inc., Cat. No.: sc-6251); rabbit anti-glucose transporter GLUT3 antibody, 1:10,000 dilution (Abcam Inc., Cat. No.: ab191071); rabbit anti-c-kit (phospho Y568 + Y570) antibody 1:10,000 dilution (Abcam Inc., Cat. No.: ab5616); rabbit anti-c-kit (phospho Y730) antibody 1:5000 dilution (Abcam Inc., Cat. No.: ab5633); goat anti-β-actin antibody, 1:1000 dilution (Santa Cruz Inc., Cat. No.: sc-1616); rabbit anti-GAPDH antibody, 1:1000 dilution (Santa Cruz Inc., Cat. No.: sc-25778). Secondary antibodies included goat anti-rabbit IgG-HRP (Santa Cruz Inc., Cat. No.: sc-2030); goat anti-mouse IgG-HRP (Santa Cruz Inc., Cat. No.: sc-2031); donkey anti-goat IgG-HRP (Santa Cruz Inc., Cat. No.: sc-2020); chicken anti-rat IgG-HRP (Santa Cruz Inc., Cat. No.: sc-2956). Secondary antibodies were used at a concentration which was half the concentration of the specific primary antibody being used.

2.8. Myocardial infarction (MI)

Acute MI was induced as previously described (Virag and Lust, 2011). Briefly, mice were anesthetized with 2% isoflurane, intubated endotracheally with a 22 gauge intravenous catheter and placed in a supine position on the warming surgery platform. Mice were ventilated using a mouse ventilator (Minivent Type845, Hugo Sachs Elektronik, Germany) to control respiration with tidal volume setting at 0.25 mL at a rate of 150 strokes/min. Prior to surgery hair was removed and the surgical area cleaned and sterilized. Subsequently, a thoracotomy was performed in the fourth intercostal space through an incision made in the left side of the chest. After displacing the pericardium, a permanent ligation of the left anterior descending artery (LAD) was conducted 2 mm below the left atrium with a 6-0 silk suture (Cat. No.: Covidien S-1750-K; esutures.com, Mokena, IL) under a dissecting microscope (Olympus SZX-7; B&B Microscopes Ltd., Pittsburgh, PA). Successful MI was verified via epicardial blanching. Following successful surgery mice were kept for 3 weeks before euthanization and organ collection.

2.9. Immunohistochemistry

Left ventricle sections were immediately fixed in 4% formaldehyde buffer solution (pH 7.2) after dissection, and paraffin embedded after 48 h of fixation. The tissues were then cut to a thickness of 4 µm and mounted onto microscopy slides. Slides were subjected to immunofluorescence staining for c-kit and CD31 in a manner similar to previous experiments (Drummond et al., 2014). The mounted paraffin embedded tissue sections were first deparaffinized with xylene and rehydrated by sequential incubations in ethanol and water. Following rehydration, antigen retrieval, blocking and antibody incubation were performed sequentially. Slides were then mounted with anti-fade gold from Life Technologies Inc. Immunofluorescence was visualized under a using confocal microscopy.

2.10. Statistical analysis

Data were presented as Mean ± SEM. One way ANOVA or t-test was used for analysis of significance.

3. Results

3.1. Intracellular expression of *c-kit* protein in isolated CDCs

We isolated CDCs from mice with a C57BL6/J background and characterized the cells based on previous publications (Smith et al., 2007; Cheng et al., 2014). Representative images of cardiac explant migration, cardiosphere formation, and amplified CDCs are shown in Fig. 1A. To further characterize the isolated CDCs, immunostaining was performed using antibodies against progenitor cell markers and different lineage markers. As shown in Fig. 1B, CDCs are positive for progenitor cell

markers such as NKx2.5, GATA4, Oct3/4 and Nanog. These cells are also CD105 positive but CD90 negative, which is consistent with published data on these cells (Smith et al., 2007; Cheng et al., 2014). In contrast, as shown in Fig. 1C, markers for endothelial cells, smooth muscle cells, and cardiomyocytes viz., CD31, α -SMA, α -actinin, and cardiac troponin I, were negative. However, CDCs were positive for the cardiac fibroblast marker, vimentin. The immunostaining in Fig. 1A was done after cell membrane permeabilization.

To check if these cells express *c-kit* and its cellular location, we used an anti-*c-kit*-FITC antibody from Abcam under conditions with or without membrane permeabilization. As shown in Fig. 2A, the fluorescent

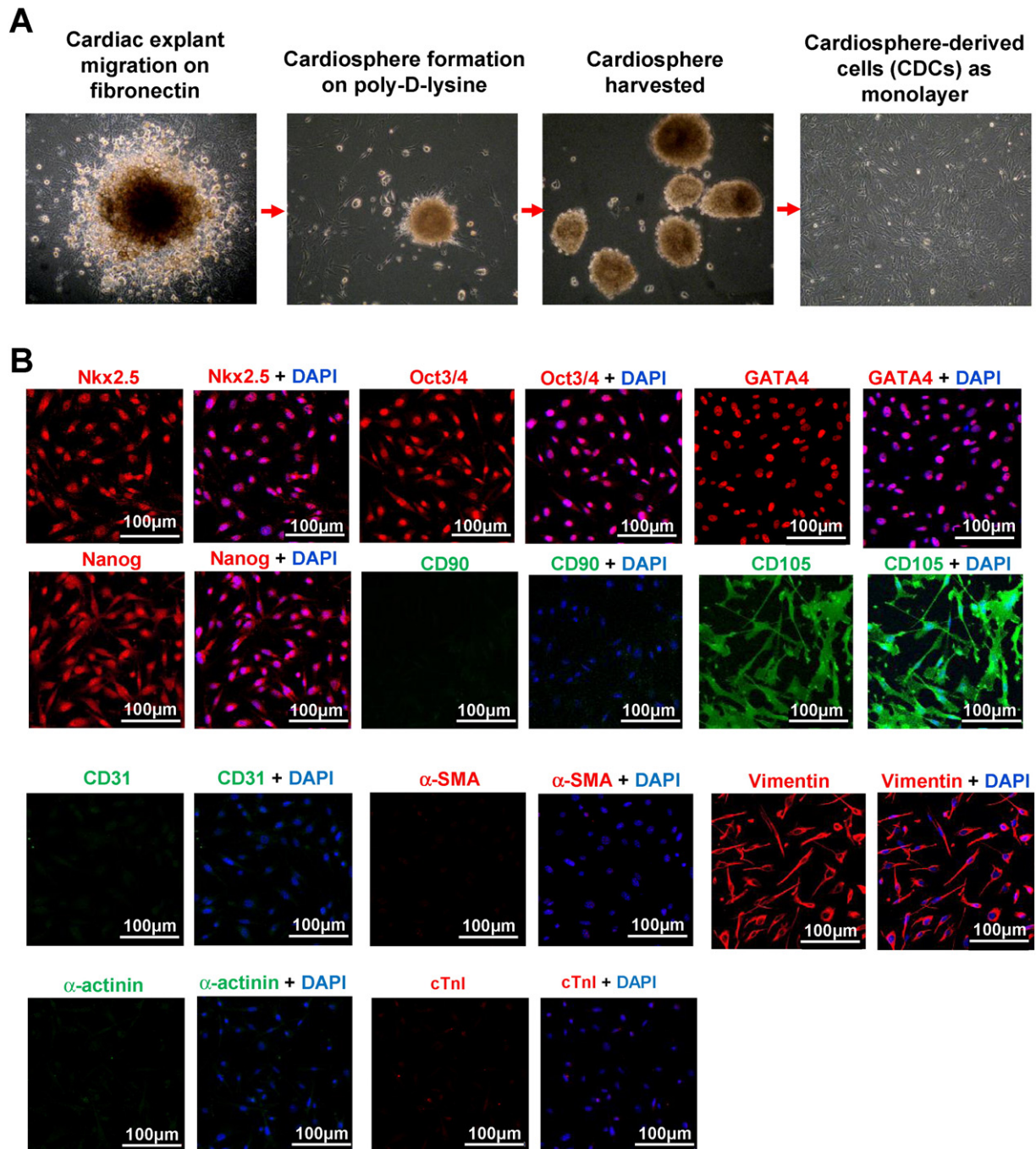


Fig. 1. Characterization of murine cardiosphere-derived cells (CDCs). (A): Shows the process of CDC isolation from 2-month old adult male mouse hearts. Cardiac muscle explants (1 mm dimension) were plated on fibronectin-coated petri dishes. Bright-phase cells migrating out of the explants were collected and seeded on poly-D-lysine coated dishes to form cardiospheres. Cardiospheres were then collected and seeded on fibronectin-coated dishes to grow as a monolayer. (B): Shows the expression of progenitor cell markers: NKx2.5, GATA4, Oct3/4, and Nanog; CDC markers reported from literature: CD90 and CD105; and different lineage markers: CD31, α -SMA, α -actinin, cardiac troponin I (cTnI), and vimentin in isolated CDCs. DAPI was used for nuclear staining in these cells.

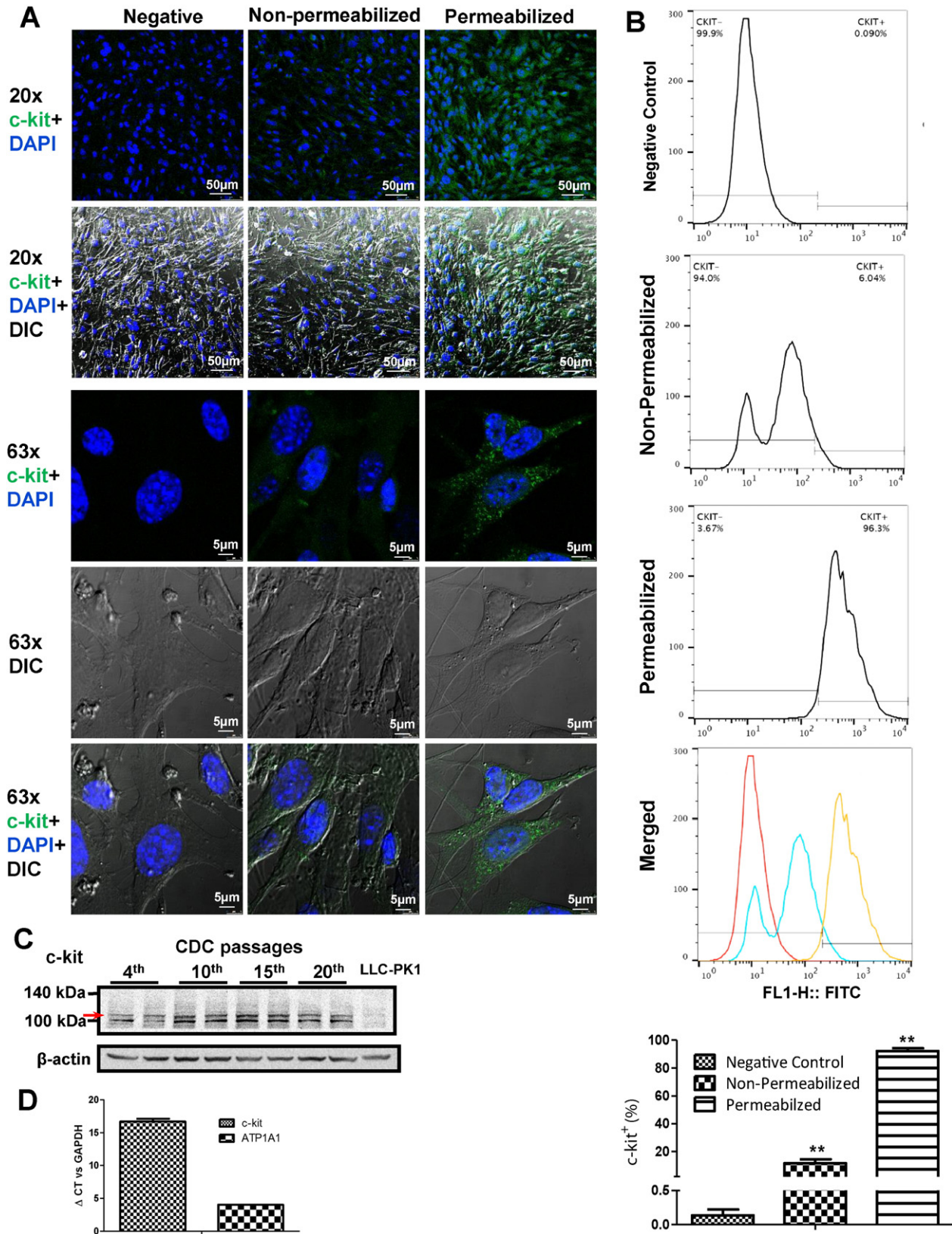


Fig. 2. Intracellular expression of c-kit in CDCs. (A): Immunostaining of c-kit in CDCs was performed using anti-c-kit-FITC antibody (the same antibody as flow cytometry). Cultured CDCs were fixed with 3% paraformaldehyde and then incubated with anti-c-kit-FITC antibody with or without membrane permeabilization. Cells which were not permeabilized and not incubated with antibody were used as negative control. Fluorescent images were taken under a Leica Confocal microscope using a 20 \times or a 63 \times lens. DAPI (purple) was used for nuclear staining; (B): Flow cytometry of CDCs indicates that a majority of c-kit expression in CDCs is intracellular. CDCs were fixed with 1.5% paraformaldehyde and stained with anti-c-kit-FITC antibody under conditions of non-permeabilization (blue curve in the merged figure) or permeabilization with 0.1% Triton X-100 (orange curve). Cells with fixation only were used as negative control (red curve); (C): Western blot of c-kit expression in CDCs in different passages. Cell lysate of CDCs were collected in RIPA buffer and probed for c-kit using Western blot. A porcine epithelial cell line, LLC-PK1, was used as negative control; (D): c-kit gene expression and Na/K-ATPase α 1 gene (Atp1a1) expression measured by qPCR, Gapdh was used as internal control. $\Delta CT_{c-kit} = CT_{c-kit} - CT_{GAPDH}$ and $\Delta CT_{ATP1A1} = CT_{ATP1A1} - CT_{GAPDH}$. Higher ΔCT means lower expression level of the gene.

signal obtained by immunostaining using this antibody was very weak in cells without membrane permeabilization, but became much stronger when cell membranes were permeabilized. Using a 63× oil lens, our results clearly show that c-kit staining was mainly intracellular (Fig. 2A). We also compared c-kit labeling using flow cytometry with or without membrane permeabilization. As shown in Fig. 2B, a population of c-kit⁺ cells with a weak fluorescent signal (peak value at 10² arbitrary units) was observed when cells were labeled without cell membrane permeabilization. However, if c-kit labeling was performed following membrane permeabilization, the fluorescent signal indicating positive c-kit staining was about 10 times higher (peak value at 10³ arbitrary units) than that in non-permeabilized cells, indicating that a vast majority of the c-kit protein was expressed intracellularly in these cells.

We also collected cell lysates from different generations of CDCs and probed for c-kit using Western blotting. A porcine proximal tubule somatic cell line (LLC-PK1) was used as negative control. As shown in Fig. 2C, CDCs express c-kit protein up to at least the 20th generation, while the negative control LLC-PK1 cells do not express c-kit protein. This result confirms that CDCs do express c-kit protein. However, the observed c-kit protein was mainly found at ~100 kDa, corresponding to a non-glycosylated form according to previous reports (Blume-Jensen et al., 1991; Rubin et al., 2001).

To further confirm the expression of c-kit in CDCs, we also performed qPCR using Gapdh as an internal control in addition to comparison with the Na/K-ATPase α 1 gene (Atp1a1), a ubiquitously expressed gene. As shown in Fig. 2D, c-kit gene expression was detected in CDCs, though at relatively low levels. This measurement, together with the immunostaining, flow cytometry, and Western blot data, clearly indicate that c-kit protein is expressed in isolated CDCs.

3.2. Endothelial differentiation increased c-kit expression and glycosylation in isolated CDCs

To examine c-kit expression and glycosylation status during differentiation, CDCs were cultured in endothelial differentiation medium as described in the “Materials and methods” section for up to 28 days while replenishing the medium every two days. Cell lysates were collected at the stem cell stage as well as at days 1, 3, 7, 10, 14, 21, and 28 after induction of endothelial differentiation. As shown in Fig. 3A, Western blot analysis showed that CDCs without differentiation induction express mainly a non-glycosylated form of c-kit found at ~100 kDa, whereas endothelial differentiation induced an additional ~140 kDa band which represents glycosylated c-kit (Rubin et al., 2001; Schmidt-Arras et al., 2005), in a time-dependent manner. The experiment also showed that endothelial differentiation induces expression of the endothelial cell markers Flk-1 and CD31 with the same pattern as glycosylated c-kit. Since c-kit glycosylation was increased after differentiation, we also probed glucose transporters. The results showed that CDCs express glucose transporter 3 (GLUT3) and its expression had a trend of increase during differentiation but was not statistically significant until 28 days after initiation of endothelial differentiation (Fig. 3A). We also probed for GLUT 1 and 4, but did not detect any changes in their expression during differentiation (data not shown).

Immunostaining using anti-c-kit-FITC antibody was performed on CDCs at different time points with membrane permeabilization. As shown in Fig. 3B, endothelial differentiation induced significant increases in c-kit as well as CD31 and Flk-1 from 7 to 14 days after induction. Fig. 3C showed high resolution images of these markers at different time points.

3.3. Inhibition of glycosylation attenuates Flk-1 and CD31 expression during endothelial differentiation in CDCs

To study if glycosylation is required for differentiation into endothelial cells, CDCs were cultured in endothelial differentiation medium with or without 1-deoxymannojirimycin hydrochloride (1-DMM), an

N-glycosylation inhibitor. Since the time course study showed the most dramatic change of c-kit glycosylation started at 7 to 14 days after differentiation induction, we chose the time point of 7 and 14 days after induction to examine the effect of 1-DMM. As shown in Fig. 4A, 1-DMM treatment reduced glycosylation of c-kit during the differentiation process. It also decreased the expression of endothelial cell markers such as Flk-1 and CD31 in these cells, but it did not affect the expression of GLUT3.

3.4. Inhibition of c-kit kinase activity by imatinib mesylate attenuated Flk-1 and CD31 expression during endothelial differentiation in CDCs

It is known that c-kit activation and phosphorylation occurs only when it becomes glycosylated (Aebi, 2013). To further test if c-kit kinase activity is required for CDC differentiation into an endothelial lineage, we treated CDCs with different concentrations of imatinib mesylate (a c-kit kinase inhibitor) during differentiation. As shown in Fig. 5, imatinib mesylate at 5 to 10 μ M reduced c-kit phosphorylation. Additionally, treatment with this kinase inhibitor also reduced Flk-1 and CD31 expression during endothelial differentiation.

3.5. C-kit⁺ cells are involved in blood vessel formation in vivo

We have shown above that CDCs can differentiate into endothelial cells, and have enhanced c-kit expression levels. To further test if c-kit expressing cells participate in the formation of blood vessels in animal models, immunostaining for c-kit and the endothelial cell marker CD31 was performed on left ventricle tissue isolated from mice subjected to myocardial infarction (MI). As shown in Fig. 6A, MI surgery significantly induced increases in c-kit cell number in addition to CD31 positive blood vessels in the infarcted zone 3 weeks following surgery. More interestingly it was found that in sham-operated mice, about 80% of the blood vessels were CD31 positive (red color) and c-kit negative (green color), while a few vessels had c-kit positive cells (upper panel of Fig. 6B). However, signals for both c-kit and CD31 were positive in most of the blood vessels in the infarcted area of heart tissue following MI in mice (lower panel of Fig. 6B), indicating that cells expressing c-kit may participate in blood vessel formation in response to MI. In these vessels, c-kit expression was seen outside the nucleus, while CD31 signal was most abundant in the junction area between neighboring cells.

4. Discussion and conclusion

4.1. Intracellular expression of c-kit is a unique feature of cardiac progenitor cells

Based on the data presented in our current study, we believe that the low abundance of membrane-associated and the immature form in which c-kit is expressed in CDCs is not a deficiency, but rather a unique feature of cardiac progenitor cells. However, a critical question that arises from this is: why does c-kit, a membrane receptor tyrosine kinase, express intracellularly in an “immature” form in CDCs? C-kit protein can be bound and activated by SCF when expressed on the plasma membrane (Lennartsson and Ronnstrand, 2012), and studies have shown that SCF stimulates cell growth in erythroid progenitor cells (Amano et al., 1993), in cerebral cortical cultures (Jin et al., 2002), and in human glioblastoma cells (Berdel et al., 1992). In our experiments, c-kit was mostly expressed in the cytosol of CDCs. Thus, c-kit in these progenitor cells likely does not function as a membrane receptor and cell growth stimulator before it commits to an endothelial lineage. In essence, these features of c-kit expression may be a unique mechanism that maintains CDC quiescence, preventing precocious responses to changes in circulating SCF. Needless to say, this hypothesis needs more sophisticated studies to be validated.

Our study revealed that the majority of CDCs express c-kit protein, suggesting that a larger population of c-kit expressing cells may exist

in cardiac tissue than previously indicated (Messina et al., 2004; Smith et al., 2007; Cheng et al., 2014). The experimental results suggest that c-kit is not only expressed in CDCs but may also directly participate in regulation of CDC differentiation. Previous characterization of CDCs found only a small population of c-kit⁺ cells (Messina et al., 2004;

Smith et al., 2007; Cheng et al., 2014). However, since c-kit protein was assumed to be a protein found on the cell surface, the determination of c-kit⁺ cell quantity was based on the method of magnetically activated cell sorting and flow cytometry without permeabilizing the cell membrane. Conversely, we used cell membrane permeabilization and

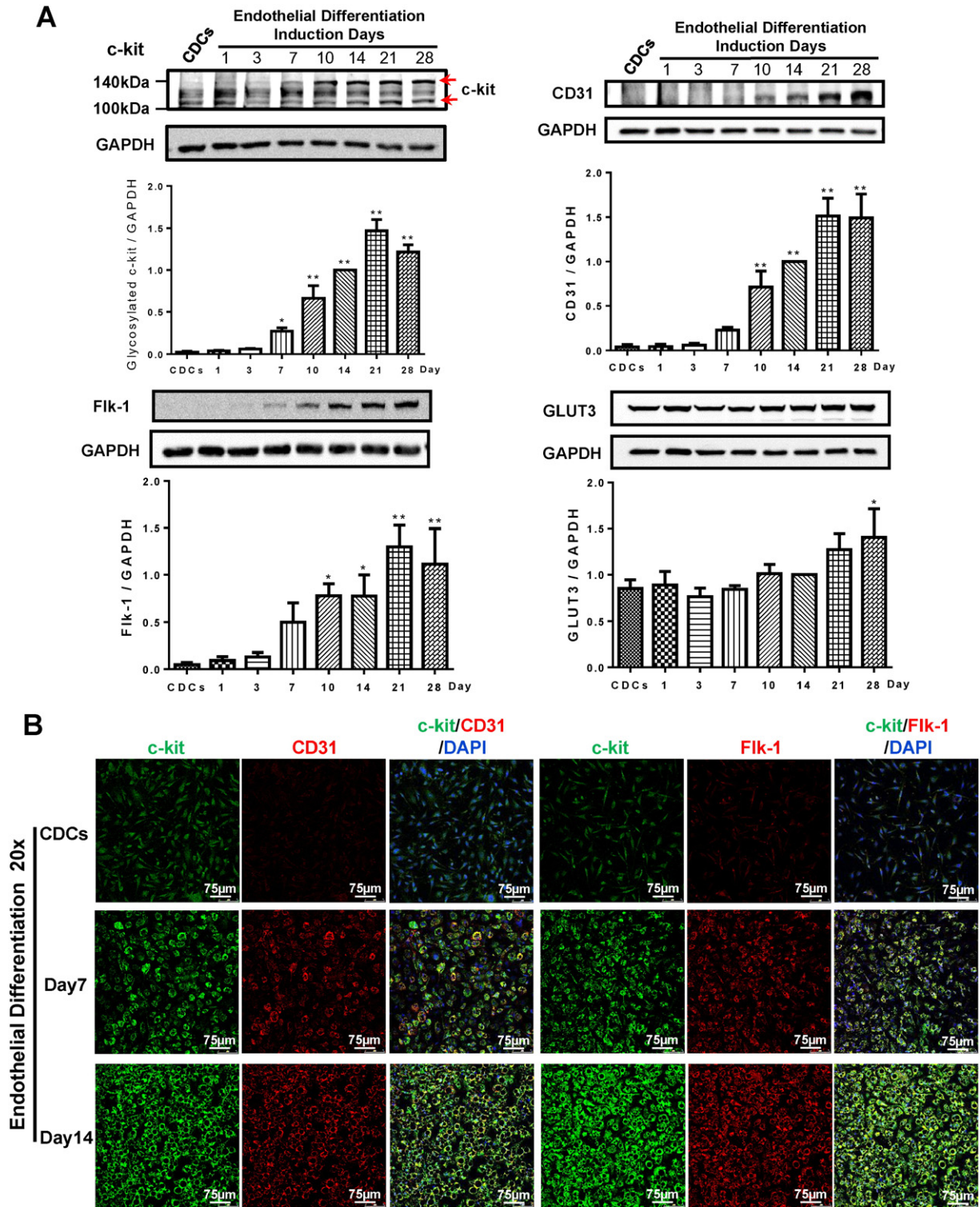


Fig. 3. Endothelial differentiation increases c-kit expression and its glycosylation in CDCs. (A): Endothelial differentiation of CDCs was initiated by changing growth medium of CDCs from CGM to MECM. Cell lysates were collected at the stem cell stage and at days 1, 3, 7, 10, 14, 21, and 28 after differentiation induction. Expression of c-kit, CD31, Flk-1, and glucose transporter 3 (GLUT3) were probed using Western blot. (B): CDCs were fixed and immunostained at the stem cell stage (before changing to differentiation medium) and at 7 and 14 days after differentiation with membrane permeabilization. Fluorescent images were taken under a Leica Confocal microscope using a 20× lens. DAPI (purple) was used for nuclear staining. (C): Higher resolution images (63× oil lens) of c-kit, CD31, and Flk-1 at different stage of differentiation. Data is presented as Mean ± SEM, n = 3 independent determinations, * indicates significant difference (p < 0.05) vs expression level at stem cell stage (CDCs), ** indicates p < 0.01.

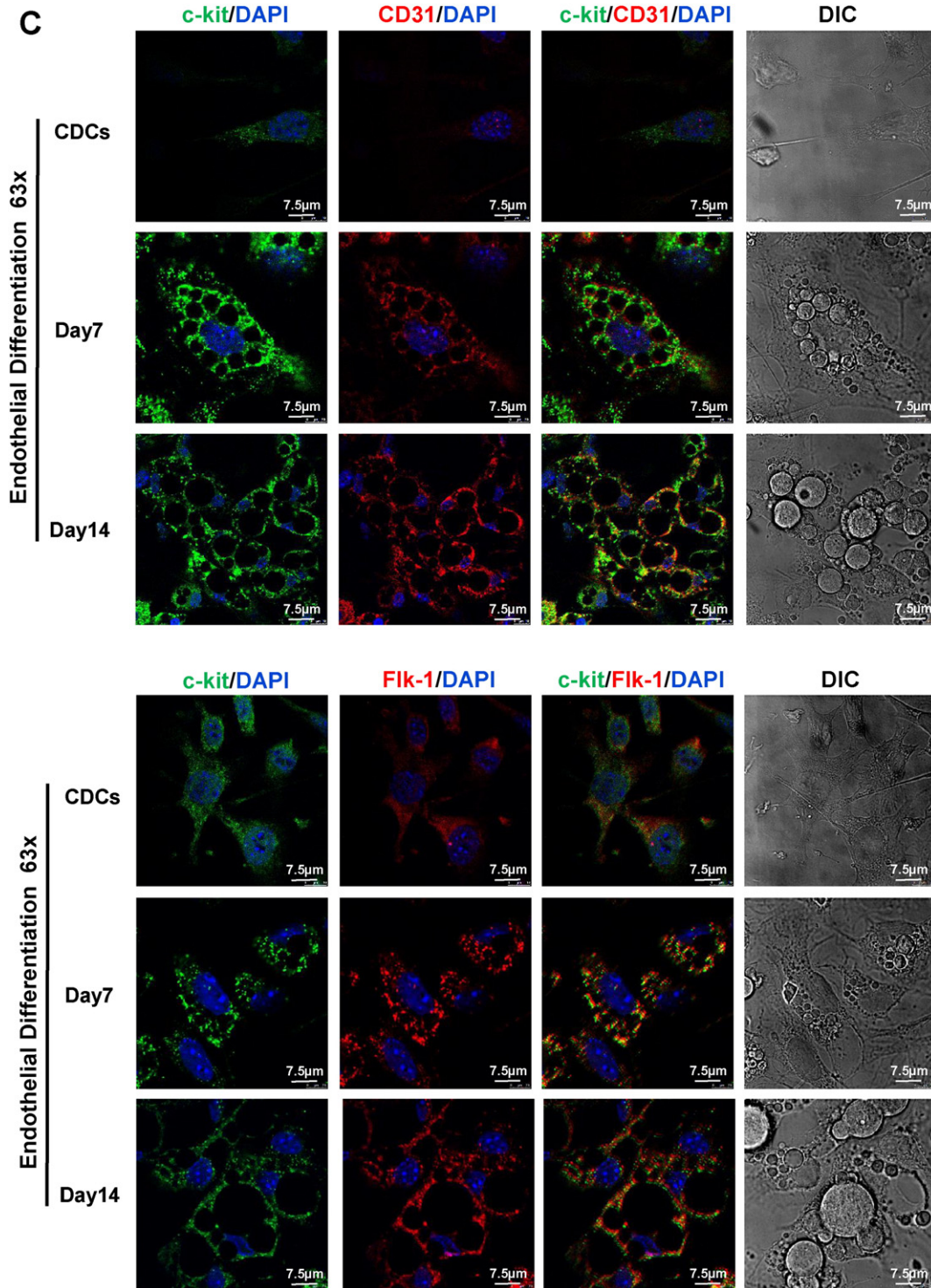


Fig. 3 (continued).

revealed that the majority of CDCs actually express intracellular c-kit protein, which is immature and non-glycosylated, and the expression can be increased and switches to the glycosylated form during endothelial differentiation. In addition, previous publications identified CDCs and c-kit⁺ cells from cardiac tissue as two separate categories of progenitor cells. Our study suggests that CDCs and c-kit⁺ cells might belong to the same population, but represent cells at different stages of activation. An early report compared the functional benefit of unsorted CDCs against magnetic bead-sorted c-kit⁺ cells and concluded that purified c-kit⁺ cells were inferior to unsorted CDCs in infarcted hearts (Li et al.,

2012). A more recent publication further showed that depletion of c-kit⁺ cells from CDCs did not affect the beneficial properties of CDCs in cardiac regeneration (Cheng et al., 2014). Given the fact that the majority of CDCs actually express intracellular c-kit protein before differentiation, based on our current study, these sorted or non-sorted cells might represent different stages of the same population of progenitor cells, which have different functional effects. Even if they represent two different populations, our results indicate that a large number of progenitor cells in cardiac tissue express c-kit protein, which can be further regulated by stimulation of differentiation. Since these new findings

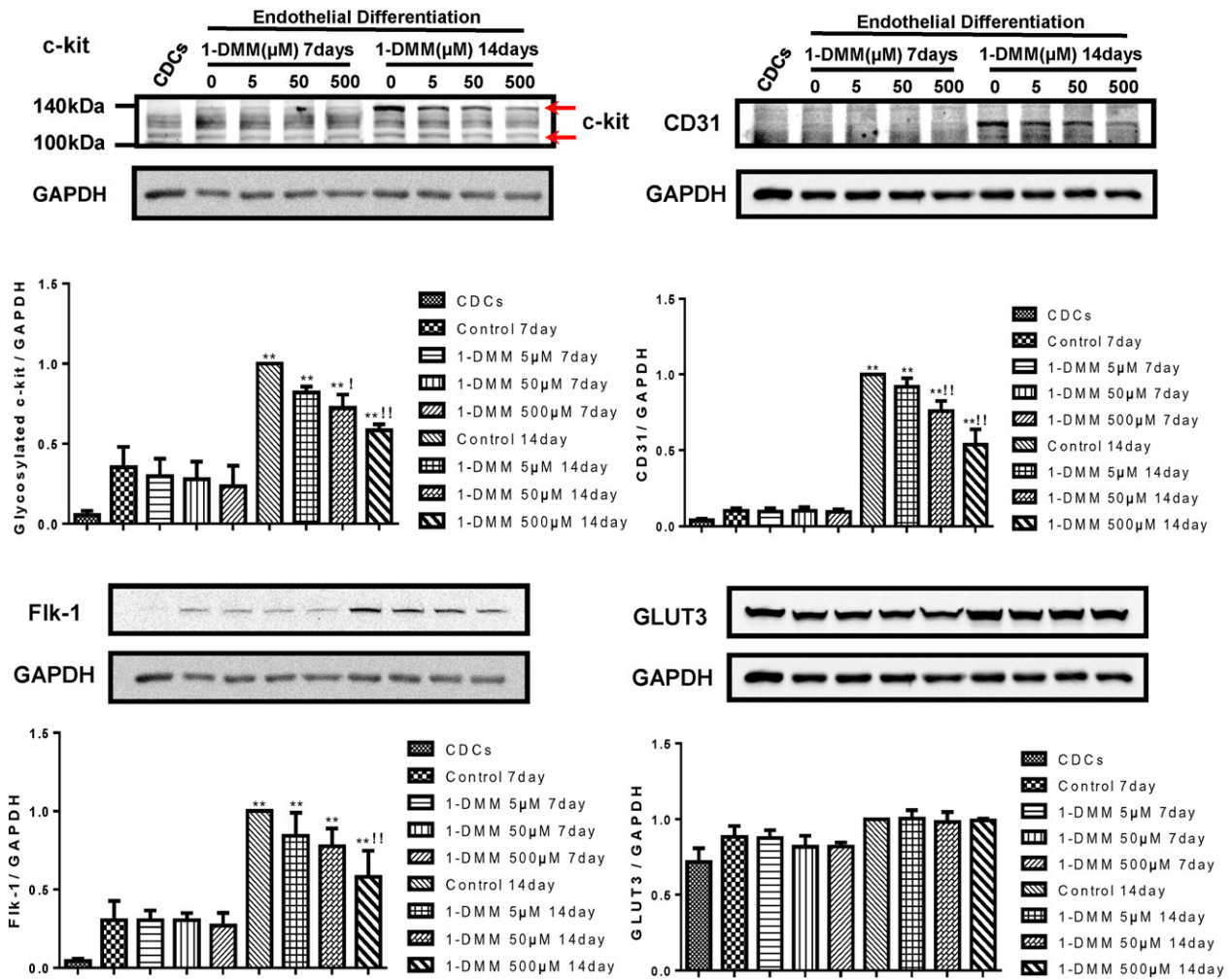


Fig. 4. Inhibition of c-kit glycosylation attenuates endothelial differentiation of CDCs. CDCs were treated with the N-glycosylation inhibitor 1-deoxymannojirimycin hydrochloride (1-DMM) at 5, 50, or 500 μM during endothelial differentiation. Cell lysates were collected 7 and 14 days following induction of endothelial differentiation to probe for c-kit, CD31, Flk-1, and GLUT3 using Western blot. Data is presented as Mean \pm SEM, n = 3 independent determinations, ** indicates significant difference ($p < 0.01$) vs expression level at stem cell stage (CDC); ! indicates significant difference ($p < 0.05$) vs control that was not treated with 1-DMM; !! indicates significant difference ($p < 0.01$) vs control that was not treated with 1-DMM.

re-characterize CDCs and re-define the population of c-kit positive cells, we suggest to call these cells “c-kit expressing progenitor cells” to distinguish from the terms that are currently used in the literature for CDCs and c-kit positive cells.

4.2. Glycosylation of c-kit may be a novel mechanism that regulates progenitor cell differentiation

C-kit has been identified as an important adult progenitor cell marker that is critical for regeneration in experimental heart failure (Nigro et al., 2015; Ellison et al., 2013). However, the exact role of c-kit in regulating progenitor cell differentiation has not been well studied. The data presented in the current study reveals that c-kit glycosylation and its kinase activity may be required for CDC differentiation into an endothelial lineage. We observed that inhibition of glycosylation by 1-DMM blocked expression of endothelial cell markers such as Flk-1 and CD31, while inhibition of c-kit kinase by imatinib mesylate also attenuates Flk-1 and CD31 expression, indicating the direct involvement of c-kit in mediating endothelial differentiation in CDCs. However, it is not clear what pathways are regulated during differentiation to trigger the glycosylation process. Our experiments showed that GLUT3 expression was increased during differentiation compared to non-differentiated CDCs. GLUT3 is a glucose transporter with high affinity to glucose and is important during embryonic development (Tonack et al., 2006).

However, the role of GLUT3 in CDC differentiation needs to be further studied.

CDCs and c-kit⁺ cells are both known to be able to differentiate into endothelial cells (Marban and Cingolani, 2012; Patruno et al., 2014; Fang et al., 2012). Our current study reveals that c-kit glycosylation is an important process during endothelial differentiation. In addition to CD31 and Flk-1, we also examined Von Willebrand Factor (VWF), a commonly used marker for endothelial cells, using Western blot and immunostaining. However, it did not show any specific signal. Given that in vitro induction of an endothelial lineage is limited in that cell display endothelial qualities and markers but are not fully functional endothelial cells, we added the in vivo examination of c-kit expressing cells. Indeed, we observed c-kit⁺ cells located within the wall of blood vessels, especially in infarcted areas of left ventricle tissue from mice subjected to MI surgery, indicating the involvement of c-kit in vascularization/angiogenesis.

In summary, the current study has re-classified the majority of the CDC population as c-kit expressing progenitor cells and demonstrated for the first time that glycosylation is an important mechanism in regulating CDC differentiation into an endothelial lineage. These results, are critical for understanding the early stages of cardiac progenitor cell regulation, and provide important information regarding the role of c-kit in cardiac progenitor cells. The finding of c-kit glycosylation and its kinase activity during CDC differentiation may serve as a potential target for

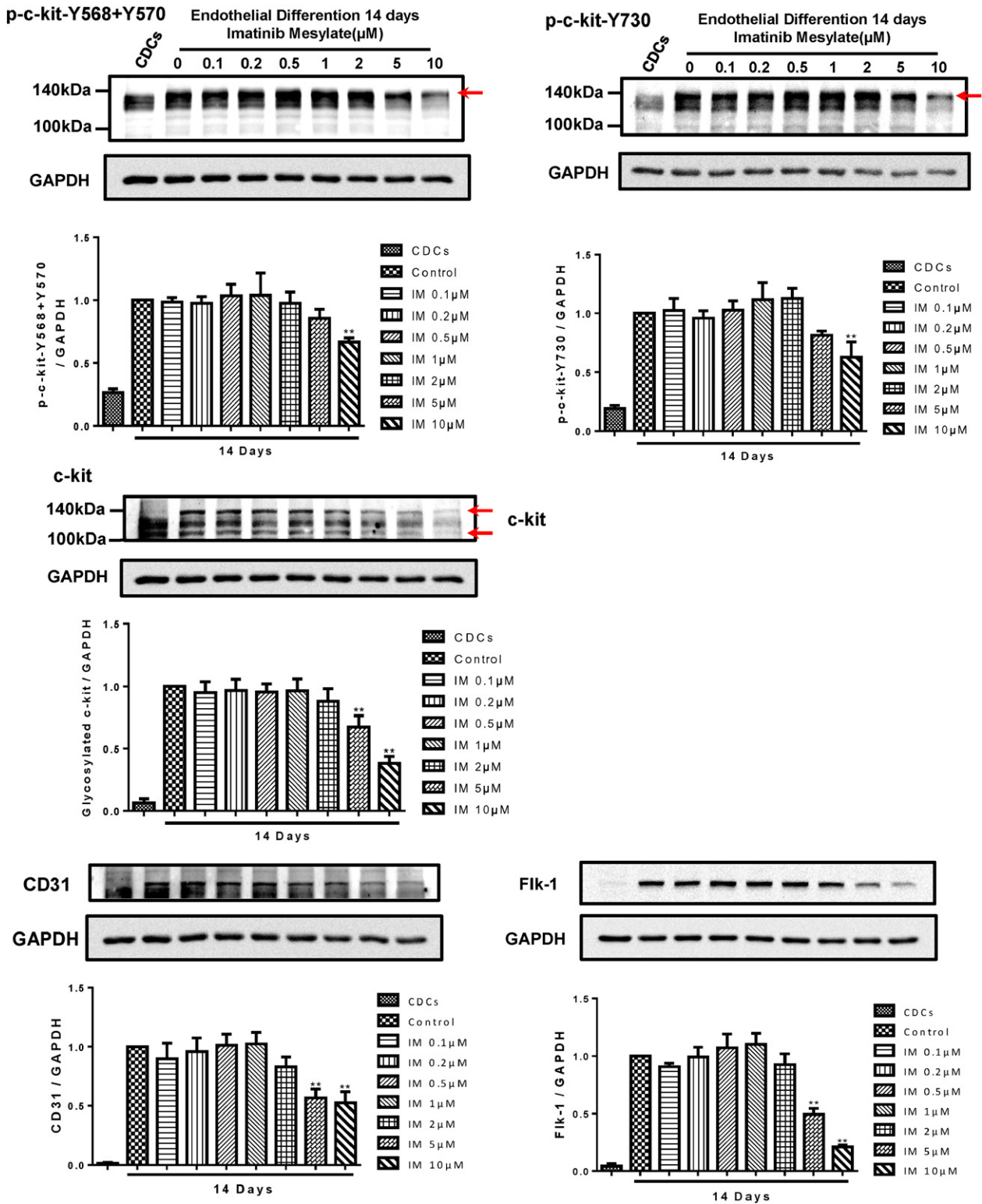


Fig. 5. The c-kit kinase inhibitor imatinib mesylate inhibits endothelial differentiation of CDCs. CDCs were treated with c-kit tyrosine kinase inhibitor imatinib mesylate at 0, 0.1, 0.2, 0.5, 1, 2, 5, or 10 μM concentrations during the 14 day endothelial differentiation induction period. Cell lysates were collected 14 days following induction of endothelial differentiation to probe for c-kit, CD31, Flk-1, phospho-c-kit (Y568 + Y570) and phospho-c-kit (Y730) using Western blot. Data is presented as Mean ± SEM, n = 3 independent determinations, ** indicates significant difference (p < 0.01) vs expression level of 14 day control.

regulating endogenous progenitor cell differentiation in disease conditions. Given the fact that direct injection progenitor cells has displayed limited potential for engrafting and low expansion efficiency in the

treatment of cardiac failure after MI (Marban, 2014), discovery of mechanisms that regulate endogenous cardiac progenitor cells are critical for future studies.

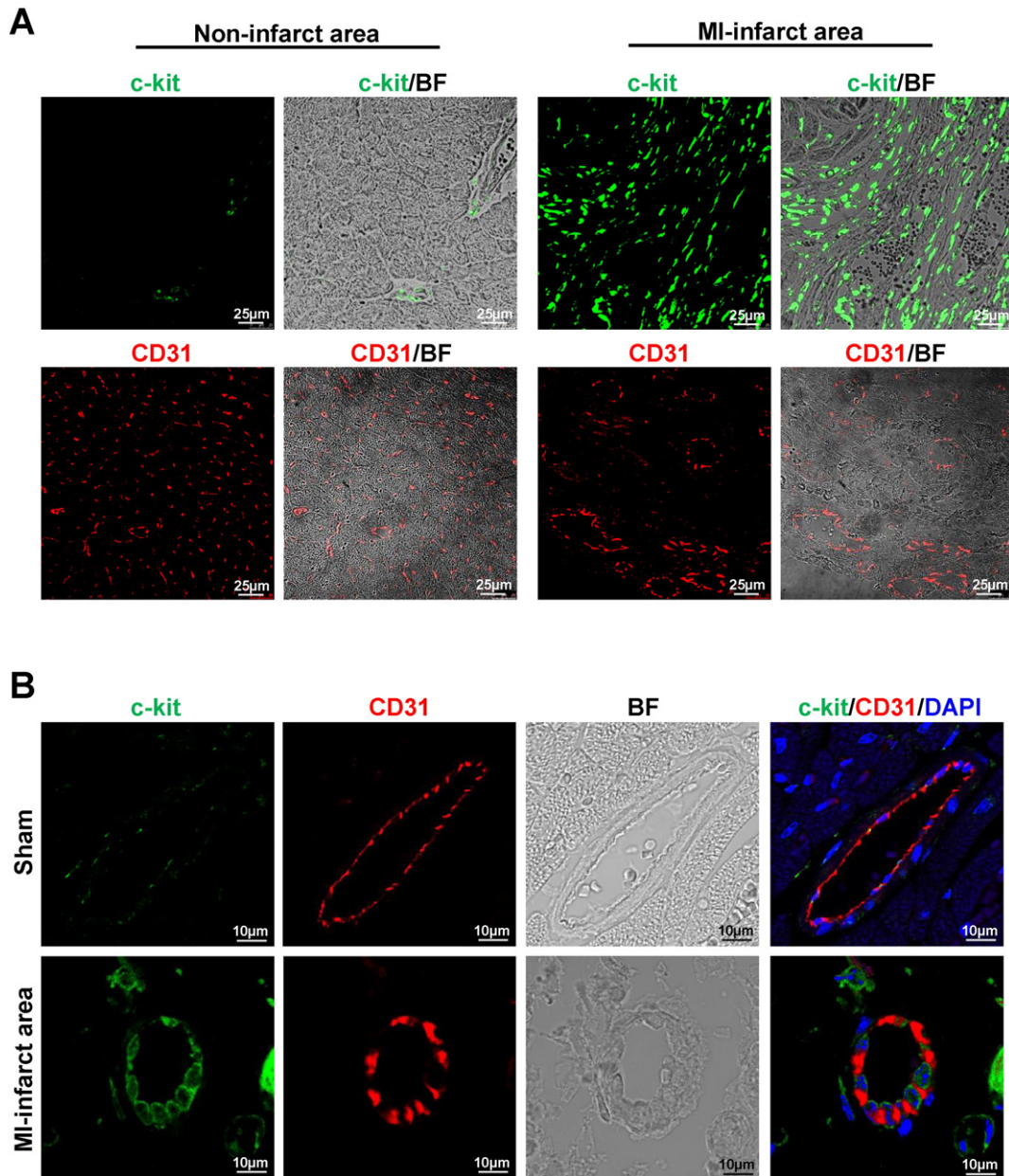


Fig. 6. The c-kit expressing cells in cardiac blood vessels after myocardial infarction in mouse heart. Mouse heart was isolated and fixed with 4% formaldehyde and immunostained with anti-c-kit-FITC antibody and anti-CD31 antibody. Fluorescence signal was visualized using a Leica Confocal microscope with 63 \times oil lens. (A): The immunostaining of c-kit and CD31 in non-infarcted area versus infarcted area. (B): Co-immunostaining of c-kit and CD31 in cardiac blood vessels from sham-operated mice (upper panel) and from the infarcted area of mice subjected to MI surgery (lower panel).

Acknowledgments

This work was supported by the National Institutes of Health (HL-105649 to JT and 1F32DK104615-01 to CAD). The cell line produced and used in this publication is freely available upon contacting the Corresponding author.

References

- Aebi, M., 2013. N-linked protein glycosylation in the ER. *Biochim. Biophys. Acta* 1833, 2430–2437.
- Amano, Y., Koike, K., Nakahata, T., 1993. Stem cell factor enhances the growth of primitive erythroid progenitors to a greater extent than interleukin-3 in patients with aplastic anaemia. *Br. J. Haematol.* 85, 663–669.
- Beltrami, A.P., Barlucchi, L., Torella, D., Baker, M., Limana, F., Chimenti, S., Kasahara, H., Rota, M., Musso, E., Urbanek, K., Leri, A., Kajstura, J., Nadal-Ginard, B., Anversa, P., 2003. Adult cardiac stem cells are multipotent and support myocardial regeneration. *Cell* 114, 763–776.
- Berdel, W.E., de Vos, S., Maurer, J., Oberberg, D., von Marschall, Z., Schroeder, J.K., Li, J., Ludwig, W.D., Kreuser, E.D., Thiel, E., et al., 1992. Recombinant human stem cell factor stimulates growth of a human glioblastoma cell line expressing c-kit protooncogene. *Cancer Res.* 52, 3498–3502.
- Besmer, P., Murphy, J.E., George, P.C., Qiu, F.H., Bergold, P.J., Lederman, L., Snyder Jr., H.W., Brodeur, D., Zuckerman, E.E., Hardy, W.D., 1986. A new acute transforming feline retrovirus and relationship of its oncogene v-kit with the protein kinase gene family. *Nature* 320, 415–421.
- Blume-Jensen, P., Claesson-Welsh, L., Siegbahn, A., Zsebo, K.M., Westermarck, B., Heldin, C.H., 1991. Activation of the human c-kit product by ligand-induced dimerization mediates circular actin reorganization and chemotaxis. *EMBO J.* 10, 4121–4128.
- Cheng, K., Ibrahim, A., Hensley, M.T., Shen, D., Sun, B., Middleton, R., Liu, W., Smith, R.R., Marban, E., 2014. Relative roles of CD90 and c-kit to the regenerative efficacy of cardiosphere-derived cells in humans and in a mouse model of myocardial infarction. *J. Am. Heart Assoc.* 3, e001260.
- Drummond, C.A., Sayed, M., Evans, K.L., Shi, H., Wang, X., Haller, S.T., Liu, J., Cooper, C.J., Xie, Z., Shapiro, J.L., Tian, J., 2014. Reduction of Na/K-ATPase affects cardiac remodeling

- and increases c-kit cell abundance in partial nephrectomized mice. *Am. J. Physiol. Heart Circ. Physiol.* 306, H1631–H1643.
- Elkareh, J., Kennedy, D.J., Yashaswi, B., Vetteth, S., Shidyak, A., Kim, E.G.R., Smaili, S., Periyasamy, S.M., Hariri, I.M., Fedorova, L., Liu, J., Wu, L., Kahaleh, M.B., Xie, Z., Malhotra, D., Fedorova, O.V., Kashkin, V.A., Bagrov, A.Y., Shapiro, J.I., 2007. Marinobufagenin stimulates fibroblast collagen production and causes fibrosis in experimental uremic cardiomyopathy. *Hypertension* 49, 215–224.
- Ellison, G.M., Torella, D., Karakikes, I., Nadal-Ginard, B., 2007. Myocyte death and renewal: modern concepts of cardiac cellular homeostasis. *Nat. Clin. Pract. Cardiovasc. Med.* 4 (Suppl. 1), S52–S59.
- Ellison, G.M., Vicinanza, C., Smith, A.J., Aquila, I., Leone, A., Waring, C.D., Henning, B.J., Stirparo, G.G., Papait, R., Scarfo, M., Agosti, V., Viglietto, G., Condorelli, G., Indolfi, C., Ottolenghi, S., Torella, D., Nadal-Ginard, B., 2013. Adult c-kit(+) cardiac stem cells are necessary and sufficient for functional cardiac regeneration and repair. *Cell* 154, 827–842.
- Fang, S., Wei, J., Pentimikko, N., Leinonen, H., Salven, P., 2012. Generation of functional blood vessels from a single c-kit+ adult vascular endothelial stem cell. *PLoS Biol.* 10, e1001407.
- Fransiolli, J., Bailey, B., Gude, N.A., Cottage, C.T., Muraski, J.A., Emmanuel, G., Wu, W., Alvarez, R., Rubio, M., Ottolenghi, S., Schaefer, E., Sussman, M.A., 2008. Evolution of the c-kit-positive cell response to pathological challenge in the myocardium. *Stem Cells* 26, 1315–1324.
- Goldstein, B.J., Goss, G.M., Hatzistergos, K.E., Rangel, E.B., Seidler, B., Saur, D., Hare, J.M., 2015. Adult c-kit(+) progenitor cells are necessary for maintenance and regeneration of olfactory neurons. *J. Comp. Neurol.* 523, 15–31.
- Hariharan, N., Quijada, P., Mohsin, S., Joyo, A., Samse, K., Monsanto, M., De La Torre, A., Avitabile, D., Ormachea, L., McGregor, M.J., Tsai, E.J., Sussman, M.A., 2015. Nucleostemin rejuvenates cardiac progenitor cells and antagonizes myocardial aging. *J. Am. Coll. Cardiol.* 65, 133–147.
- Jin, K., Mao, X.O., Sun, Y., Xie, L., Greenberg, D.A., 2002. Stem cell factor stimulates neurogenesis in vitro and in vivo. *J. Clin. Invest.* 110, 311–319.
- Lennartsson, J., Ronnstrand, L., 2012. Stem cell factor receptor/c-kit: from basic science to clinical implications. *Physiol. Rev.* 92, 1619–1649.
- Leri, A., Rota, M., Pasqualini, F.S., Goichberg, P., Anversa, P., 2015. Origin of cardiomyocytes in the adult heart. *Circ. Res.* 116, 150–166.
- Li, Z., Zhang, Z., Xie, J.X., Li, X., Tian, J., Cai, T., Cui, H., Ding, H., Shapiro, J.I., Xie, Z., 2011. Na/K-ATPase mimetic pNaKtide peptide inhibits the growth of human cancer cells. *J. Biol. Chem.* 286, 32394–32403.
- Li, T.S., Cheng, K., Malliaras, K., Smith, R.R., Zhang, Y., Sun, B., Matsushita, N., Blusztajn, A., Terrovitis, J., Kusuoka, H., Marban, L., Marban, E., 2012. Direct comparison of different stem cell types and subpopulations reveals superior paracrine potency and myocardial repair efficacy with cardiosphere-derived cells. *J. Am. Coll. Cardiol.* 59, 942–953.
- Makkar, R.R., Smith, R.R., Cheng, K., Malliaras, K., Thomson, L.E., Berman, D., Czer, L.S., Marban, L., Mendizabal, A., Johnston, P.V., Russell, S.D., Schuleri, K.H., Lardo, A.C., Gerstenblith, G., Marban, E., 2012. Intracoronary cardiosphere-derived cells for heart regeneration after myocardial infarction (CADUCEUS): a prospective, randomised phase 1 trial. *Lancet* 379, 895–904.
- Marban, E., 2014. Breakthroughs in cell therapy for heart disease: focus on cardiosphere-derived cells. *Mayo Clin. Proc.* 89, 850–858.
- Marban, E., Cingolani, E., 2012. Heart to heart: cardiospheres for myocardial regeneration. *Heart Rhythm* 9, 1727–1731.
- Mercola, M., Ruiz-Lozano, P., Schneider, M.D., 2011. Cardiac muscle regeneration: lessons from development. *Genes Dev.* 25, 299–309.
- Messina, E., De Angelis, L., Frati, G., Morrone, S., Chimenti, S., Fiordaliso, F., Salio, M., Battaglia, M., Latronico, M.V., Coletta, M., Vivarelli, E., Frati, L., Cossu, G., Giacomello, A., 2004. Isolation and expansion of adult cardiac stem cells from human and murine heart. *Circ. Res.* 95, 911–921.
- Moseley, A.E., Coughnon, M.H., Grupp, I.L., El Schultz, J., Lingrel, J.B., 2004. Attenuation of cardiac contractility in Na,K-ATPase alpha1 isoform-deficient hearts under reduced calcium conditions. *J. Mol. Cell. Cardiol.* 37, 913–919.
- Nigro, P., Perrucci, G.L., Gowran, A., Zanobini, M., Capogrossi, M.C., Pompilio, G., 2015. c-Kit(+) cells: the tell-tale heart of cardiac regeneration? *Cell. Mol. Life Sci.* 72, 1725–1740.
- Olson, E.N., Schneider, M.D., 2003. Sizing up the heart: development redux in disease. *Genes Dev.* 17, 1937–1956.
- Patruno, R., Marech, I., Zizzo, N., Ammendola, M., Nardulli, P., Gadaleta, C., Inrona, M., Capriuolo, G., Rubini, R.A., Ribatti, D., Gadaleta, C.D., Ranieri, G., 2014. c-Kit expression, angiogenesis, and grading in canine mast cell tumour: a unique model to study c-kit driven human malignancies. *BioMed Res. Int.* 2014, 730246.
- Rubin, B.P., Singer, S., Tsao, C., Duensing, A., Lux, M.L., Ruiz, R., Hibbard, M.K., Chen, C.J., Xiao, S., Tuveson, D.A., Demetri, G.D., Fletcher, C.D., Fletcher, J.A., 2001. KIT activation is a ubiquitous feature of gastrointestinal stromal tumors. *Cancer Res.* 61, 8118–8121.
- Schmidt-Arras, D.E., Bohmer, A., Markova, B., Choudhary, C., Serve, H., Bohmer, F.D., 2005. Tyrosine phosphorylation regulates maturation of receptor tyrosine kinases. *Mol. Cell. Biol.* 25, 3690–3703.
- Smith, R.R., Barile, L., Cho, H.C., Leppo, M.K., Hare, J.M., Messina, E., Giacomello, A., Abraham, M.R., Marban, E., 2007. Regenerative potential of cardiosphere-derived cells expanded from percutaneous endomyocardial biopsy specimens. *Circulation* 115, 896–908.
- Tonack, S., Rolletschek, A., Wobus, A.M., Fischer, B., Santos, A.N., 2006. Differential expression of glucose transporter isoforms during embryonic stem cell differentiation. *Differentiation* 74, 499–509.
- van Berlo, J.H., Kanisicak, O., Maillet, M., Vagnozzi, R.J., Karch, J., Lin, S.C., Middleton, R.C., Marban, E., Molkenkin, J.D., 2014. c-Kit+ cells minimally contribute cardiomyocytes to the heart. *Nature* 509, 337–341.
- Virag, J.A., Lust, R.M., 2011. Coronary artery ligation and intramyocardial injection in a murine model of infarction. *J. Vis. Exp.* JoVE, e2581.
- Yarden, Y., Kuang, W.J., Yang-Feng, T., Coussens, L., Munemitsu, S., Dull, T.J., Chen, E., Schlessinger, J., Francke, U., Ullrich, A., 1987. Human proto-oncogene c-kit: a new cell surface receptor tyrosine kinase for an unidentified ligand. *EMBO J.* 6, 3341–3351.